Effects of rapid thermal annealing on the morphology and optical property of ultrathin InSb film deposited on SiO_2/Si substrate*

Li Deng-Yue(李邓玥)†, Li Hong-Tao(李洪涛), Sun He-Hui(孙合辉), and Zhao Lian-Cheng(赵连城)

Department of Information Materials Science and Technology, Harbin Institute of Technology, Harbin 150001, *China*

(Received 11 May 2012; revised manuscript received 25 July 2012)

Ultrathin InSb films on SiO_2/Si substrates are prepared by radio frequency (RF) magnetron sputtering and rapid thermal annealing (RTA) at 300, 400, and 500 °C, respectively. X-ray diffraction (XRD) indicates that InSb film treated by RTA at 500 °C, which is higher than its melting temperature (about 485 °C), shows a monocrystalline-like feature. A high-resolution transmission electron microscopy (HRTEM) micrograph shows that melt recrystallization of InSb film on SiO_2/Si (111) substrate is along the (111) planes. The transmittances of InSb films decrease and the optical band gaps redshift from 0.24 eV to 0.19 eV with annealing temperature increasing from 300 °C to 500 °C, which is indicated by Fourier transform infrared spectroscopy (FTIR) measurement. The observed changes demonstrate that RTA is a viable technique for improving characteristics of InSb films, especially the melt-recrystallized film treated by RTA at 500 °C.

Keywords: XOI, solid-phase recrystallization, rapid thermal annealing

PACS: 78.40.Fy, 43.35.Ns, 68.60.Bs **DOI:** 10.1088/1674-1056/22/2/027802

1. Introduction

Moore's law has predicted that the number of transistors, which are placed inexpensively on an integrated circuit, doubles approximately every two years. This trend is expected to be maintained until at least 2020. Nowadays the 65-nm technology node of the most advanced microprocessors in production has a transistor gate length of 35 nm, which is likely to be 22 nm in 2016.[1,2] Over the past several years, the inherent scaling limitations of electron devices bring many technical challenges from the traditional work mode, i.e. material and basic device physics, therefore researchers should promptly overcome or improve some of these challenges with various research breakthroughs. Ultrathin III–V compound semiconductor film growth on Si-based substrate has attracted significant attention because of the combination of the high mobility of III–V semiconductors and the well-established, low-cost processing of Si technology. In parallel with silicon-on-insulator (SOI) technology, XOI was used to represent the compound semiconductor-on-insulator platform.[3–6] InSb has the smallest effective mass, the narrowest band gap, and the highest intrinsic electron mobility of III–V semiconductors. Solid-phase crystallization using low-temperature furnace annealing (FA) requires very long annealing time and hence suffers from a substantial tradeoff between performance and throughput. This problem can be solved by using the rapid thermal annealing (RTA) technique.[7] In the state-of-the-art RTA processing an infrared lamp-based programmable computer-controlled system is utilized. Benefits of RTA processing include a reduction of the energy or thermal budget, a shorter processing time, and the ability to precisely control the temperature profile that the device sees.

In this paper, ultrathin InSb films are grown on SiO_2/Si (111) substrates using RF magnetron sputtering and then solid-phase recrystallization by RTA treatment at different temperatures. The remainder of this paper is organized as follows. To begin, we describe the detailed deposition process of 35-nm InSb film on SiO_2/Si (111) substrate. Then the morphology, structures, and optical properties of ultrathin InSb films on SiO_2/Si are presented. Finally, we conclude that with the increase of annealing temperature, the InSb film crystalline quality becomes better. The transmittance and the value of the optical band gap decreases with the rise of annealing temperature.

2. Experimental details

Si substrates each with a dimension of about 20 mm × 20 mm × 0.6 mm are cut from mirror polished p-type Si (111) wafers. The resistivity of each substrate at room temperature is about 20 Ω·cm. Substrates are first chemically cleaned in the RCA procedure[8] then thermally oxidized at 800 °C with dry O_2 gas of 99.999% purity and less than 1 ppmv of H_2O for 10 min to obtain an SiO_2 thickness of about 40 Å (1 Å = 0.1 nm) on each substrate.

InSb films are deposited on SiO_2/Si (111) substrate at room temperature by RF magnetron sputtering using an InSb alloy target. The base pressure is 10^{-6} Pa to ensure a low level of impurities. The growing conditions are 55-W RF power, 0.6-Pa Ar pressure to ensure good crystallographic properties. The deposition experiments show that when a stoichiometric polycrystalline InSb target is used, the film is rich in indium

*Project supported by the Special Funds for State 11th Five-Year Basic Research Project of China (Grant No. 51318060207).

†Corresponding author. E-mail: dyli2012@126.com

© 2013 Chinese Physical Society and IOP Publishing Ltd

and the excess indium is presented on the surface of the film in the form of indium balls. This is usually explained by the relatively large equilibrium vapor pressure of group V metals in comparison with that of the group III metals. In this study with a purity of 99.9995% antimony (Sb) and 99.9995% of indium (In), the InSb template is made by the water-cooled copper crucible in a vacuum arc furnace in an argon atmosphere. After being confined, rod-like samples are suction-casted into a size of 10 mm (diameter) × 75 mm (length). Using wire cutting, the rod is cut into suitably shaped specimens, cleaned with acetone, then sealed into a quartz tube under a vacuum pressure of 10^{-2} Pa, kept for 24 hours at 450 °C to achieve uniformity of composition. The composition of each specimen is determined by energy spectrum technique. The In/Sb ratio in the film is also measured, and after measuring more than 30 samples, it is found that the film with an atom ratio of 1:1 is grown by the target with a ratio of 1:0.82.

Post-deposition thermal annealing of the film is accomplished in an N_2 atmosphere using a rapid photothermal annealing system, i.e., RTA. The samples are annealed at 300, 400, 500 °C for 4 minutes, respectively. The typical ramp-up and ramp-down temperatures are both ∼20 °C/s. The accuracy of temperature measurement is ±2 °C.

X-ray diffraction (XRD), high-resolution transmission electron microscopy (HRTEM), and transmission electron microscopy (TEM) are used to study the crystallographic microstructure and the film thickness, respectively. The powder XRD pattern is recorded on a Philip X'Pert Discover (Cu Ka radiation, $\lambda = 1.5406$ Å), and the scanning range is from 20° to 80°. Cross-sectional TEM and HRTEM image are recorded on a JEOL JEM 2010F field emission electron microscope, using an accelerating voltage of 200 kV.

Fourier transform infrared spectroscopy (FTIR) measurement is carried out by a Perkin Elmer Lamda 2000 spectrum in transmittance mode at room temperature in a spectral range between 2.5 μm and 25 μm, and the SiO_2/Si wafer is used as the reference.

3. Results and discussion

InSb films are annealed by RTA at various temperatures ranging from 300 °C to 500 °C. Figure 1 shows XRD patterns of both as-deposited InSb films and films after RTA treatment at different temperatures on SiO_2/Si (111) substrates. It is clear that the temperature of RTA plays an important role in the crystallization of InSb film. No diffraction peak is observed in the as-deposited sample, demonstrating the typical behavior of amorphous or disordered material.[9] As seen in Fig. 1 (curve *b*), sample (b) is found to be polycrystalline, but the intensity of the InSb (111) peak is larger than that of the other InSb-related peak. In Fig. 1 (curve *c*), the intensity of the InSb-related peak visibly increases compared with sample (b) especially the InSb (111) peak. In contrast to the samples annealed at lower temperatures, sample (d), which is annealed at 500 °C, (which is higher than the melting temperature of InSb film of about 485 °C),[10] shows an obviously single crystalline-like feature, and the other InSb-related peaks are very weak. According to Eq. (1)[11]

$$\alpha(111) = \frac{I(111)}{I(111)+I(110)} \times 100\%, \tag{1}$$

where α is the orientation degree, and $I(111)$ and $I(110)$ are the intensities of peaks (111) and (110), respectively. It is found that the orientation degree α of peak (111) of InSb film annealed at 300 °C by RTA treatment is about 0.62. However, as the temperature increases to 400 °C, the orientation degree α of peak (111) increases to about 0.71. The orientation degree α of peak (111) is nearly 1 after being melt-recrystallized and treated by RTA at 500 °C. That means that the melt-recrystallized InSb film treated by RTA at 500 °C shows a preferred (111) orientation. Pelleg *et al.*[12] reported that the preferred orientation is considered as a result of the competition between surface and strain energy which is based on the frequently observed "orientation crossover". In the present study, the thicknesses of all these films deposited on SiO_2/Si substrates are almost the same, therefore, the difference in stress between these films can be neglected, and the films? growth is determined by the surface energy. For low-index planes, the relation of the surface energy γ is $\gamma(110) < \gamma(111)$, therefore, melt-recrystallized InSb film treated by RTA at 500 °C may gain more energies than the films annealed at lower temperatures, which leads to (111) preferred orientation. This result indicates that with the increase of annealing temperature, the crystalline quality of InSb film improves. The melt-recrystallized InSb film treated by RTA at 500 °C obtains a good crystalline quality.

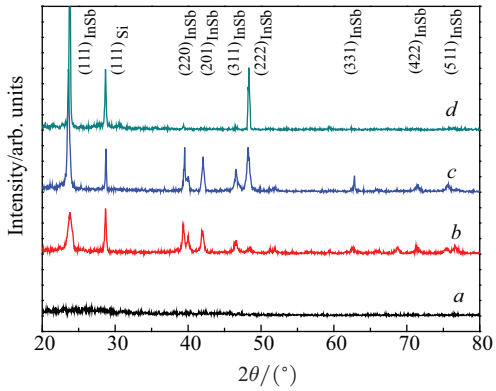


Fig. 1. (color online) X-ray patterns of InSb films (curve *a*) as-deposited, and after RTA treatments at (curve *b*) 300 °C, (curve *c*) 400 °C, (curve *d*) 500 °C on SiO_2/Si (111) substrates.

Figure 2 shows the variations of grain size and full width at half maximum (FWHM) of InSb film treated by RTA with

temperature. Each XRD peak is carefully measured, and the grain size is calculated by the Scherr formula,[13]

$$D = 0.9\lambda / B\cos\theta, \tag{2}$$

where λ is the wavelength of the X-ray radiation (λ = 0.154 nm), B is the full width at half maximum (FWHM) of the peak (in radians) corrected for instrumental broadening, θ is the Bragg angle and D is the crystallite size. The grain size of InSb film increases with annealing temperature increasing, because enhanced crystallinity of the film reduces the FWHM of the (111) peak. From the present experimental observations, we conclude that the annealing-induced crystallinity improvement in InSb film structure occurs at a higher annealing temperature. It indicates that the annealing treatment could increase the activation energy of crystallization. The crystal quality of InSb film is improved by RTA treatment and melt recrystallization at 500 °C.

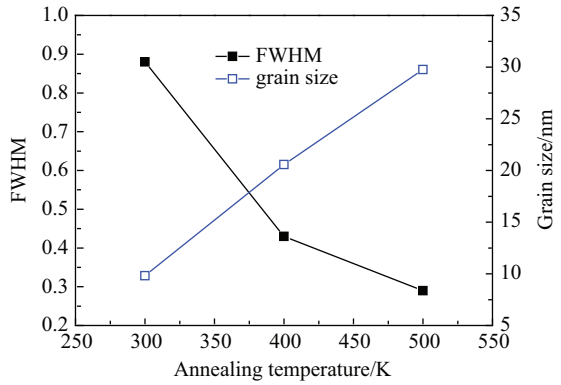


Fig. 2. (color online) FWHM and grain size of InSb films versus annealing temperature.

HRTEM images of both (a) as-deposited InSb films and after RTA treatment at (b) 300 °C, (c) 400 °C, and (d) 500 °C on SiO_2/Si (111) substrate, are presented in Fig. 3, respectively. As shown in Fig. 3(a), the as-deposited InSb film demonstrates the typical behavior of amorphous or disordered material which is consistent with the result from the XRD pattern in Fig. 1(a). Because the InSb layer and the SiO_2 layer are both of amorphous phase, the InSb/SiO_2 interface is difficult to find from the image. A TEM image of InSb film is shown in the inset of Fig. 3(a), the thickness of the deposited InSb layer is about 35 nm. As shown in Fig. 3(b), after RTA treatment at 300 °C, InSb film exhibits an obvious polycrystalline structure. The InSb/SiO_2 interface is clearer than the as-deposited InSb/SiO_2 interface. The InSb film under RTA treatment at 400 °C also exhibits a polycrystalline structure but the crystallinity of the film is improved which is shown in Fig. 3(c). The interface between InSb and SiO_2 is clearly found in the HRTEM image.

Figure 3(d) shows a relatively sharp interface and clear lattice fringes after melt recrystallization and RTA treatment at 500 °C. The most interesting finding is that the amorphous InSb film on SiO_2/Si substrate is converted into a well-ordered crystal structure. This observation indicates that a suitable annealing temperature constitutes a crystalline InSb on SiO_2/Si substrate, i.e., the energy barrier for crystallization can be overcome by supplying sufficient kinetic energy of melt recrystallization at 500 °C, resulting in a well-ordered crystalline InSb on SiO_2/Si substrate. The lattice fringe between two adjacent planes is about 3.75 Å, indicating that the melt recrystallization of InSb film on SiO_2/Si (111) substrate is along the (111) plane. Evidently, the HRTEM analysis here is in good agreement with the XRD data discussed above.

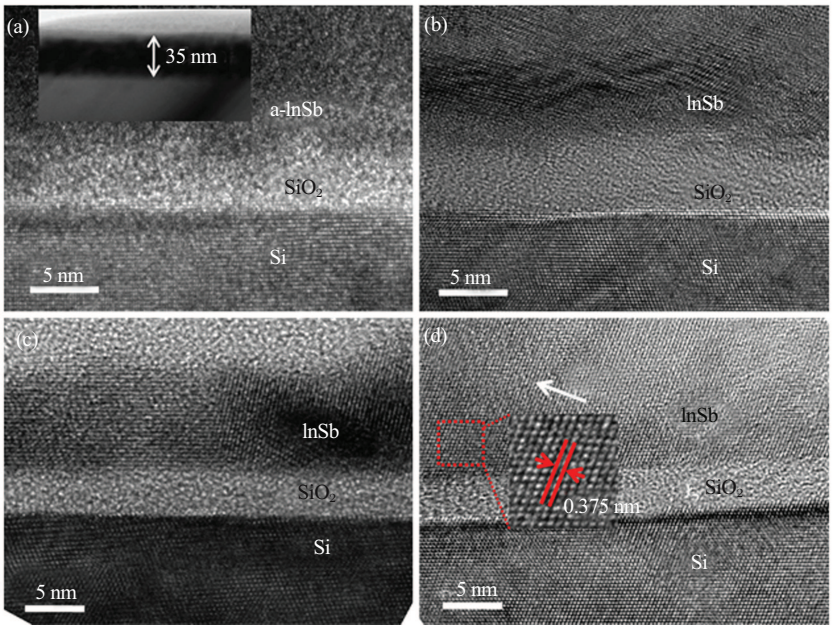


Fig. 3. (color online) HRTEM images of InSb films (a) as-deposited, with the inset showing the cross-sectional TEM image of InSb film, and after RTA treatments at (b) 300 °C, (c) 400 °C, (d) 500 °C on SiO_2/Si (111) substrates.

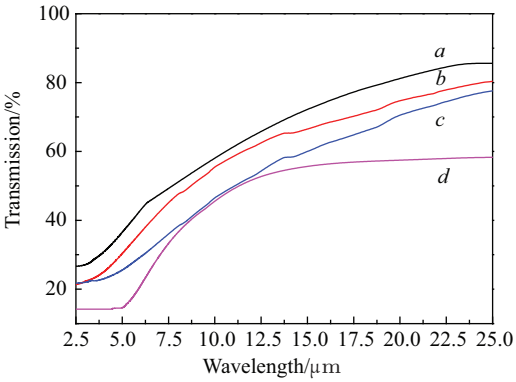


Fig. 4. (color online) Curves of transmission versus wavelength of InSb films (curve *a*) as-deposited, and after RTA treatments at 300 °C (curve *b*), (curve *c*) 400 °C, (curve *d*) 500 °C on SiO_2/Si (111) substrates.

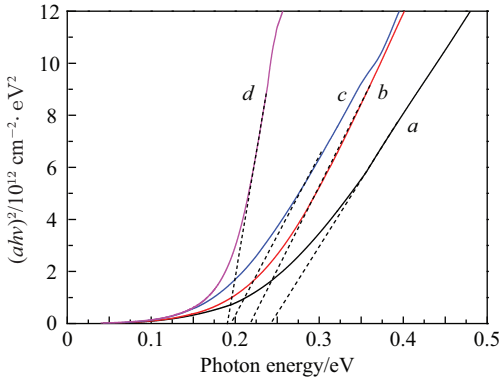


Fig. 5. (color online) Curves of $(\alpha h\nu)^2$ versus photon energy of InSb films (curve *a*) as-deposited, and after RTA treatments at 300 °C (curve *b*), 400 °C (curve *c*) and 500 °C (curve *d*) on SiO_2/Si (111) substrates.

Figure 4 illustrates the spectral transmittances of the films annealed by RTA treatment at different temperatures from 300 °C to 500 °C. It can be seen from Fig. 4 that the transmittances of the films decrease with annealing temperature increasing. It means that the samples annealed at higher temperatures are more absorbable. We can also see that the absorption edges shift toward longer wavelength as the annealing temperature increases. This phenomenon can be observed clearly in Fig. 5, which shows the dependence of the absorption coefficient on photon energy. The optical band gap energy of the film is obtained by using the Tauc model[14] in the high absorbance region,

$$\alpha h\nu = D(h\nu - E_g)^n, \tag{3}$$

where α is the absorption coefficient, $h\nu$ is the photon energy, E_g is the optical band gap, and D is a constant. It can be found that $n = 2$ corresponds to a semiconductor of the indirect transition type and $n = 1/2$ leads to a semiconductor of the direct transition type.[15] Following the conventional method of extrapolating the linear part of the Tauc plot, the optical band gap energies for direct transition for the InSb films that are as-deposited and RTA treated at different temperatures are obtained directly from the absorption spectrum as shown in Fig. 5. The optical band gap of the as-deposited film is found to be 0.24 eV. For the samples annealed by RTA, the optical band gaps redshift from 0.24 °C to 0.19 eV with annealing temperature increasing from 300 °C to 500 °C. Vasantkumar and Mansingh[16] suggested that the decrease in band gap energy with the increase of temperature is due to the lowering of interatomic spacing (amorphous to crystalline).

4. Conclusions

In this paper, we grow ultrathin InSb films on SiO_2/Si (111) substrates. The films are solid-phase recrystallized at different temperatures by RTA treatment. Our results indicate a significant correlation between the temperature of RTA treatment and the property of ultrathin InSb film. The film shows a monocrystalline-like feature for the InSb film treated by RTA at 500 °C, which is higher than its melting temperature (about 485 °C), and the value of the optical band gap decreases with annealing temperature rising.

References

[1] Moore G E 2003 *IEEE International Solid-State Circuits Conference*, February 9–13, 2003, San Francisco, CA, USA, pp. 20–23
[2] Robert C, Brian D, Suman D, Jack K and Kevin Z 2007 *Nat. Mater* **6** 810
[3] Ko H, Takei K, Kapadia R, Chuang S, Fang H, Leu P W, Ganapathi K, Plis E, Kim H S, Chen S Y, Madsen M, Ford A C, Chueh Y L, Krishna S and Salahuddin S 2010 *Nature* **468** 286
[4] Ford A C, Yeung C W, Chuang S, Kim H S, Plis E, Krishna S, Hu C M and Javey A 2011 *Appl. Phys. Lett.* **98** 113105
[5] Fang H, Madsen M, Carraro C, Takei K, Kim H S, Plis E, Chen S Y, Krishna S, Chueh Y L, Maboudian R and Javey A 2011 *Appl. Phys. Lett.* **98** 012111
[6] Rogers J A 2010 *Nature* **468** 177
[7] Ma Z H, Cao Q, Zuo Y H, Zheng J, Xue C L, Cheng B W and Wang Q M 2011 *Chin. Phys.* **20** 106104
[8] Kern W and Puotinen D A 1970 *RCA Rev.* **31** 187
[9] Motemani Y, Tan M J, White T J and Huang W M 2011 *Materials and Design* **32** 688
[10] Shuichi O, Kazuhiko A and Daisuke E 2008 *Appl. Phys. Lett.* **92** 011919
[11] Liu H, Gong X G, Zhang Z N, Wang Z H, Huang H D, Li Y R, Xiao D Q and Zhu J G 2007 *Ferroelectrics* **357** 259
[12] Pelleg J, Zevin L Z and Lungo N 1991 *Thin Solid Films* **197** 117
[13] Cullity B D 1978 *Elements of X-ray Diffraction* 2nd edn. (Reading Mass: Addison-Wesley Publishing Company) pp. 162–166
[14] Tauc J 1974 *Amorphous and Liquid Semiconductors* (London: Plenum) pp. 159–176
[15] Ohkubo S, Aoki K and Eto D 2008 *Appl. Phys. Lett.* **92** 011919
[16] Vasantkumar C V R and Mansingh A 1990 *Seventh IEEE International Symposium on Application of Ferroelectrics* (New York: IEEE) pp. 713–716